

not necessarily the same as the μ -mesons commonly observed in cosmic rays. If there were the " μ -mesons" which constitute π -mesons, as suggested by Wenzel, the production of the " μ -mesons" in a high energy nucleon-nucleon collision ($\sim 10^{12}$ ev) is estimated by the statistical theory of Fermi¹⁹ to be as large as that of π -mesons. Such " μ -mesons" should give a large contribution to the total intensity of cosmic rays at great depths and their intensity-depth relation would be considerably different from that of ordinary μ -

¹⁹ E. Fermi, *Prog. Theor. Phys.* **5**, 570 (1950).

mesons, since the effect of the decay process is quite important. The allowable fraction of undelayed particles at the depth under consideration is so small⁵ that the existence of the hypothetical " μ -mesons" may be ruled out. As far as the experimental evidences underground thus far obtained are concerned, the introduction of new particles and new interactions seems to be unnecessary.

It is my great pleasure to express my hearty thanks to Professors Cocconi and Greisen, and Drs. Bollinger and Cocconi Tongiorgi for the communication of their experimental results and their stimulating discussions.

The High Energy Nuclear Photoeffect

J. S. LEVINGER*

Cornell University, Ithaca, New York

(Received March 29, 1951)

The nuclear photoeffect for photons of energy greater than 150 Mev is calculated assuming the two-nucleon model used by Heidmann. The main features of the nuclear photoeffect are then quite similar to those of the deuteron photoeffect. The cross section for nuclear absorption of a high energy photon is about 1.6A times the cross section for the deuteron photoeffect. The deuteron photoeffect gives a very strongly forward angular distribution for protons of a given energy, observed in the laboratory system. The angular distribution for protons from the nuclear photoeffect is almost as strongly forward: for 90-Mev protons in the laboratory system the ratio of the differential cross section at 60° to that at 90° is about 3. The proton energy spectrum decreases rapidly with proton energy, and becomes steeper for observations at large angles. The calculated angular distributions and proton energy spectra are in fair agreement with measurements by Walker. The absolute value of the differential cross section for 90-Mev protons from carbon at 30° (laboratory system) is about 0.2 μ barn/Mev steradian per Q , or about 20 μ barn/steradian per photon. This absolute value is about one-third the absolute value measured by Walker, and is somewhat larger than the absolute value measured by Levinthal and Silverman.

I. INTRODUCTION

RECENT experiments by Levinthal and Silverman,¹ Keck,² Walker,³ and Kikuchi⁴ have shown the production of high energy protons from nuclei irradiated by high energy photons. Protons up to energies of at least 150 Mev were produced by the bremsstrahlung photon spectra of the 300-Mev Berkeley and Cornell synchrotrons. Nuclear cross sections are of the order of 0.1 millibarn. The angular distribution of the emitted protons showed a marked forward asymmetry in the laboratory system, particularly for the higher energy protons.

At low excitation energies the compound nucleus picture has been successful. The compound nucleus picture fails to explain these observations at high excitation energies in two respects: (1) it predicts that very few high energy nucleons will be emitted; (2) it predicts an isotropic angular distribution. In fact, the

compound nucleus model fails to explain the ratio of cross sections for (γ, p) and (γ, n) processes,⁵ and angular distributions for emitted protons,⁶ at intermediate excitation energies (17.5 Mev). Courant⁷ interprets the (γ, p) processes at these intermediate energies as a direct photoelectric emission of protons. He uses two different models: (1) independent proton wave functions in a square well potential; (2) an approximate alpha-particle model. Somewhat better agreement with experimental results is found with the second model.

At extremely high excitation energies we might regard each nucleon in the nucleus as independent. High energy protons might be produced by independent Compton scattering by each proton in the nucleus. The cross section for this process is much smaller than that observed experimentally for the production of high energy protons.

Another possible mechanism for the photoproduction of high energy protons is via the production of photo-

* Now at Louisiana State University, Baton Rouge, Louisiana.

¹ C. Levinthal and A. Silverman, *Phys. Rev.* **82**, 822 (1951).

² J. Keck (private communication).

³ D. Walker, *Phys. Rev.* **81**, 634 (1951).

⁴ S. Kikuchi, *Phys. Rev.* **80**, 492 (1950).

⁵ O. Hirzel and H. Wäffler, *Helv. Phys. Acta* **20**, 373 (1947).

⁶ B. C. Diven and G. M. Almy, *Phys. Rev.* **80**, 407 (1950).

⁷ E. D. Courant, *Phys. Rev.* **82**, 703 (1951).

mesons (either neutral or charged). The π -meson might subsequently be absorbed by another nucleon in the same nucleus, giving a star that might contain a high energy proton. This process would show a smaller forward asymmetry for proton production than was observed; so it cannot be the major process for production of high energy protons. It might be significant at large angles, where the process discussed below gives a very small cross section.

For the nuclear photoeffect by photons of energy greater than about 150 Mev we shall use a nuclear model intermediate between the compound nucleus model and the independent nucleon model: i.e., we assume the nuclear wave function to be the product of the wave function for two nucleons very close together with a wave function for the remaining nucleons. This two-nucleon model has been used by Tamor⁸ in calculating the production of high energy protons following capture of π^- mesons. Tamor also used an alpha-particle model. Experimental results⁹ are in better agreement with Tamor's calculations for the alpha-particle model. The two-nucleon model has been applied by Heidmann¹⁰ to the pick-up reaction for high energy (90-Mev) neutrons. He finds reasonable agreement with York's measurements¹¹ on the production of fast deuterons by 90-Mev neutrons.

One might expect to use a similar model for the production of fast protons by π^- capture, for the pick-up reaction, and for the high energy nuclear photoeffect. In all three reactions the proton has a high momentum in the final state and, since it cannot gain much momentum in the reactions considered, it must have had a high momentum in the ground state. A proton will have a high momentum (far above that for the most energetic proton in a Fermi gas of nuclear density) if it is acted on by strong forces due to being very near other nucleons. If the distance from the proton to its nearest neighbor is much smaller than the average spacing of nucleons in the nucleus (1.4×10^{-13} cm), then it is likely that no other nucleons will be similarly near to the two nucleons which are very close together. Since small nucleon distances correspond to high nucleon momenta, the two-nucleon model should become more valid for very high momentum components of the ground-state nuclear wave function: i.e., for high energies of the emitted proton.¹²

Levinthal and Silverman¹ also reach the conclusion

⁸ S. Tamor, Phys. Rev. **77**, 412 (1950).

⁹ W. B. Cheston and L. J. B. Goldfarb, Phys. Rev. **78**, 683 (1950).

¹⁰ J. Heidmann, Phys. Rev. **80**, 171 (1950).

¹¹ H. F. York, Phys. Rev. **75**, 1467 (1949).

¹² We are making an additional assumption that the potential between two nucleons increases rapidly with decreasing distances, for distances somewhat smaller than 1.4×10^{-13} cm. This assumption is valid for an exponential or a Yukawa potential, but not for a gaussian or square-well potential. Neutron-proton scattering experiments are in agreement with the first two potentials, but not with the last two. For the last two, the high momentum components of the potential, and hence of the wave function, would be too small to explain the high energy photoeffect.

that high momentum components of the ground state wave function are responsible for the high energy photoeffect. (They use a mathematical argument to reach this conclusion, rather than the physical argument made above.) Chew and Goldberger¹³ found an empirical momentum distribution to fit York's measurements¹¹ on the neutron pick-up reaction. Levinthal and Silverman use this empirical momentum distribution to find the cross section for the high energy photoeffect, and find approximate agreement with their experimental data. In principle there is no essential difference between their approach and ours; the difference is only one of method. Because of the absence of a model, their calculation gives no information on the angular distribution of the high energy protons.

Since we are using a two-nucleon, or deuteron model, many of the features of the high energy photoeffect are determined by those for the high energy photodisintegration of the deuteron. Schiff,¹⁴ and Marshall and Guth,¹⁵ (called SMG below) have calculated the deuteron photoeffect for photon energies from 20 to 140 Mev. They find that the electric dipole term provides almost all of the total photoelectric cross section; while interference between the electric dipole and the electric quadrupole interactions produces forward asymmetry for the proton angular distribution in the center-of-mass system.

The remaining $A-2$ nucleons in the nucleus will affect our results in two ways: they constitute a potential well in which the deuteron moves; and they may scatter the high energy nucleons. In this paper we shall be concerned with small nuclei (carbon) and as a first approximation neglect the effects of scattering by the other nucleons.

In Sec. II we calculate the ratio of the cross section for the high energy nuclear photoeffect to that for the deuteron photoeffect. In Sec. III we compare the high energy photoeffect with the calculated nuclear cross section for photon absorption integrated over all photon energies.¹⁶ In Sec. IV we calculate the energy spectrum and the angular distribution (laboratory system) for protons and neutrons from photodisintegration of the deuteron. In Sec. V we find the energy spectrum and angular distribution for protons from the photodisintegration of carbon. In the last section we compare our calculations with recent experimental results.

II. THE DEUTERON MODEL

Since a proton-proton system has no dipole moment, and the dipole term in the photoelectric effect is predominant at the photon energies considered, we need consider only proton-neutron systems. The two-nucleon model becomes a deuteron model, for the high energy

¹³ G. F. Chew and M. L. Goldberger, Phys. Rev. **77**, 470 (1950).

¹⁴ L. I. Schiff, Phys. Rev. **78**, 733 (1950).

¹⁵ J. F. Marshall and E. Guth, Phys. Rev. **78**, 738 (1950).

¹⁶ J. S. Levinger and H. A. Bethe, Phys. Rev. **78**, 115 (1950).

photoeffect. The nuclear deuterons can be in either a triplet S state (probability $\frac{3}{4}$) or a singlet S state (probability $\frac{1}{4}$).¹⁷ SMG's results apply exactly only for the triplet S state, but since our calculation is rather approximate, we shall use their results for both cases. Also the quasi-deuterons in the nucleus do not have a binding energy of 2.2 Mev; on the contrary, the proton and neutron have a positive energy, due to motions of nucleons in the nucleus. However, as shown below, the wave function of the quasi-deuteron, for the neutron and proton very close together, is a multiple of the wave function of the deuteron; so that the photodisintegration cross section for sufficiently high energies is that given by SMG for the deuteron, multiplied by a suitable factor.

Following Heidmann¹⁰ we write the wave function for the ground state of the nucleus, with proton 1 very close to neutron 2, as

$$\Psi(1, 2, 3 \cdots A) = \exp(i\mathbf{k}' \cdot \mathbf{r}') \psi_k(r) \varphi(3 \cdots A). \quad (1)$$

The term $\exp(i\mathbf{k}' \cdot \mathbf{r}')$ represents the motion of the center of mass of the quasi-deuteron. We shall assume that the wave function φ for the remaining $A-2$ nucleons is the same for both initial and final states.¹⁸ The cross section for the production of high energy protons will then depend only on the quasi-deuteron wave function $\psi_k(r)$, where r is the distance between the proton and neutron. This function can be written

$$\psi_k(r) = (4\pi)^{\frac{1}{2}} [\sin(kr + \delta) / \sin \delta - \chi] / (\alpha^2 + k^2)^{\frac{1}{2}} v^{\frac{1}{2}}. \quad (2)$$

χ is a function which is appreciable only inside the range of the nuclear forces and depends on the shape of the potential. Further, v is the volume of the nucleus, and k is the wave number for the relative motion of proton and neutron given by

$$k = \frac{1}{2} |\mathbf{k}_1 - \mathbf{k}_2|. \quad (3)$$

\mathbf{k}_1 and \mathbf{k}_2 are wave numbers for proton and neutron when they are far from each other. From the theory of the effective range of nuclear forces^{19,20} the phase shift δ is given approximately by

$$\cot \delta \cong -\alpha/k. \quad (4)$$

α^{-1} is the scattering length. The wave function of Eq. (2) becomes the S term of a plane wave for r larger than the range of nuclear forces. The plane wave is normalized so that integration over r gives one proton per volume v surrounding the neutron. (We are assuming that the nuclear density is constant.)

For the high energy photoeffect we are interested primarily in the behavior of ψ_k at small r where $kr \ll 1$.

¹⁷ We are interested only in S states, because only for these states are the neutron and proton likely to be very close together.

¹⁸ This assumption will in general overestimate the cross section, since the overlap integral for φ will be unity or less.

¹⁹ H. A. Bethe, Phys. Rev. **76**, 38 (1949).

²⁰ H. A. Bethe and C. Longmire, Phys. Rev. **77**, 647 (1950).

Expanding Eq. (2), and using Eq. (4) we have

$$\begin{aligned} \psi_k(r) &= (4\pi/v)^{\frac{1}{2}} (\alpha^2 + k^2)^{-\frac{1}{2}} r^{-1} [-(\alpha/k) \sin kr + \cos kr - \chi] \\ &\cong (4\pi/v)^{\frac{1}{2}} (\alpha^2 + k^2)^{-\frac{1}{2}} r^{-1} (1 - \alpha r - \chi). \end{aligned} \quad (5)$$

The wave function of the deuteron ground state is

$$\begin{aligned} \psi_d(r) &= [2\alpha/(1 - \alpha r_0)]^{\frac{1}{2}} r^{-1} (e^{-\alpha r} - \chi) \\ &\cong [2\alpha/(1 - \alpha r_0)]^{\frac{1}{2}} r^{-1} (1 - \alpha r - \chi), \end{aligned} \quad (6)$$

which follows from the theory of the effective range. (r_0 is the effective range.) In that theory it is shown that both the comparison function (asymptotic behavior for large r , there^{19,20} denoted by ψ , in our case $\exp(-\alpha r)$) and the actual wave function in the potential (there called u , in our case $e^{-\alpha r} - \chi$) are very insensitive to the energy of the deuteron, as long as r is inside the range of nuclear forces. This is the reason why the wave functions given in Eq. (2) and Eq. (6) are proportional to each other in the relevant region of small r . For the photoelectric cross section of the quasi-deuteron we can then simply use the SMG result for the deuteron which must be multiplied by the ratio of the squares of the constant, or normalization factors in Eq. (5) and Eq. (6) giving

$$\sigma_{qd}/\sigma_d = (\psi_k/\psi_d)^2 = 2\pi(1 - \alpha r_0)/\alpha(\alpha^2 + k^2)v. \quad (7)$$

Here σ_{qd} is the photodisintegration cross section for a quasi-deuteron in which the neutron and proton have wave number k for their relative motion; and σ_d is the SMG result for the deuteron. Since have Z choices for proton 1, and N choices for neutron 2 ($N = A - Z$), the nuclear cross section is $NZ\sigma_{qd}$.

We must also average $(\alpha^2 + k^2)^{-1}$ over all possible values of the wave number k . We assume Fermi distributions for proton wave number k_1 , and neutron wave number k_2 , up to the same maximum wave number k_m .

$$P(k_1) dk_1 = (3/k_m^3) k_1^2 dk_1, \quad k_1 \leq k_m. \quad (8)$$

We also assume an isotropic distribution for the angle between \mathbf{k}_1 and \mathbf{k}_2 . Using Eq. (3) for the value of k , we find

$$\begin{aligned} [(\alpha^2 + k^2)^{-1}]_N &= 9k_m^{-2} - 24\alpha k_m^{-3} \tan^{-1}(k_m/\alpha) \\ &\quad - 6\alpha^2 k_m^{-4} + (18\alpha^2 k_m^{-4} + 6\alpha^4 k_m^{-6}) \\ &\quad \times \ln(1 + k_m^2 \alpha^{-2}) = 4.1 k_m^{-2}. \end{aligned} \quad (9)$$

The numerical result is found using $\alpha = 0.23 \times 10^{13} \text{ cm}^{-1}$, and $k_m = 1.0 \times 10^{13} \text{ cm}^{-1}$.

Equation (9) is substituted in Eq. (7). We shall take the volume of the nucleus as $v = (4/3)\pi A (1.4 \times 10^{-3})^3$, and multiply by NZ as discussed above. The cross section for photodisintegration of the nucleus becomes

$$\sigma = 6.4(NZ/A)\sigma_d \cong 1.6A\sigma_d. \quad (10)$$

The second expression holds for $N = Z = A/2$. Our result should be valid for high photon energies, say, greater than 150 Mev, and is expected to overestimate the nuclear cross section for lower photon energies.

III. COMPARISON WITH INTEGRATED CROSS SECTIONS

It is of interest to note that the proportionality to the quantity NZ/A (or approximately to A) which we have already found for the nuclear cross section for high energy photons, using the deuteron model, is just the same as the dependence of the dipole term in the nuclear absorption cross section integrated over photons of all energy.¹⁶ (W is photon energy.)

$$\int_0^{\infty} \sigma dW = (2\pi^2 e^2 \hbar / Mc)(NZ/A)(1+0.8x) \cong 0.015A(1+0.8x) \text{ Mev barns.} \quad (11)$$

Here x is the fraction of attractive exchange force. The coefficient 0.8 depended somewhat on the nuclear model used; but except for this the result was completely independent of the nuclear model.²¹

We shall use the calculations by SMG for a Yukawa potential between neutron and proton. They assume exactly half ordinary and half exchange force ($x = \frac{1}{2}$), so that there is no force in the P state which is reached by dipole transitions. (A larger fraction of ordinary force would lower the high energy photodisintegration cross section; a larger fraction of exchange force would increase it.)

The dipole term σ_1 for deuteron photodisintegration calculated by SMG can be written²²

$$\sigma_1 = [1 - y^2(44 + y)^{-2}]^2 \sigma_B / (1 - \alpha r_0). \quad (12)$$

Here $\sigma_B / (1 - \alpha r_0)$ is the Bethe-Peierls cross section, corrected using effective range theory,²⁰ and $y =$ photon energy/binding energy of deuteron. To compare the cross section for the high energy nuclear photoeffect, with that integrated over all energies, we integrate Eq. (12) over photon energies from 220 Mev (chosen arbitrarily) to infinity, and use Eq. (10). We find that the integrated nuclear cross section is

$$\int_{220}^{\infty} \sigma_1 dW = 0.0029A \text{ Mev barn.} \quad (13)$$

This is 14 percent of the cross section integrated over all photon energies found from Eq. (11), using the value $x = \frac{1}{2}$, to correspond to SMG's calculations. Thus the high energy photoeffect is a small but not negligible part of the integrated photon absorption cross section.

The "tail" caused by the high energy photoeffect has a much larger effect on the mean energy \bar{W} for photon absorption. By integrating Eq. (12) we find that

$$\int_{220}^{\infty} \sigma_1 W dW = 0.68A \text{ Mev}^2 \text{ barn.} \quad (14)$$

²¹ However the theoretical result for the mean energy \bar{W} is increased appreciably by the correlation involved in the use of the deuteron model for the high energy photoeffect. This can be seen from Eq. (27) of reference 16.

²² See also J. S. Levinger, Phys. Rev. **76**, 699 (1949), with $\beta/\alpha = 6.7$.

Defining $\Delta\bar{W}$ as the increase in the mean absorption energy due to the high energy tail, we have

$$\Delta\bar{W} = \int_{220}^{\infty} \sigma_1 W dW / \int_0^{\infty} \sigma_1 dW = 32 \text{ Mev.} \quad (15)$$

Since the high energy tail has such a large effect on the mean energy for photon absorption (assuming that the deuteron model calculation is correct) one cannot find reliable values of \bar{W} from measurements at only moderate photon energies. Johns *et al.*,²³ for example, have determined values of the integrated cross section and the mean energy \bar{W} for certain photonuclear reactions. Since their measurements extend only up to photon energies of 26 Mev, the cross section integrated up to infinite photon energy is appreciable higher than their measured value, and the mean energy is very much higher than their measured value.

IV. THE DEUTERON PHOTOEFFECT

In this section we shall give the energy spectrum and angular distribution for protons, and neutrons, produced by photodisintegration of the deuteron. In the following section we shall calculate how these distributions are modified for protons and neutrons produced from heavier nuclei. The work of this section consists principally of transformation of the SMG results for the center of mass system to distributions in the laboratory system.

SMG calculate the deuteron photoeffect for a Yukawa potential between neutron and proton, half exchange and half ordinary in character, of effective range 1.74×10^{-13} cm. They have calculated the photoelectric dipole and quadrupole cross sections. SMG give their results only up to photon energies of 150 Mev, since they believe that mesonic effects, such as increased photomagnetic cross sections due to exchange currents, will have a marked effect at high photon energies.²⁴ Also, higher electric multipoles start becoming appreciable at higher energies. Since our whole calculation is rather approximate, we shall use the formulas of SMG up to photon energies of 300 Mev.

The high energy photodisintegration of the deuteron gives a strongly forward angular distribution for the emitted protons for three reasons, about equal in their effects. First, as discussed by SMG, interference between electric dipole and electric quadrupole matrix elements is constructive in the forward hemisphere (CM system) and destructive in the backwards hemisphere, for emitted protons. (For emitted neutrons the distribution will be backwards in the CM system.) Second, the forward motion of the CM system relative to the laboratory system, due to the photon momentum, shifts the angular distribution forward. Third, measure-

²³ Johns, Katz, Douglas, and Haslam, Phys. Rev. **80**, 1062 (1950).

²⁴ Photomagnetic transitions will be especially important for observations at angles near 0° and near 180° , where the photoelectric cross sections vanish.

ments made for fixed proton energy (laboratory system) favor protons emitted forward, since these protons were produced by lower energy photons than were protons of the same energy that were emitted backward. Here we make use of the fact that the cross section for the photoeffect and the photon intensity (for the bremsstrahlung spectrum) both decrease with increasing photon energy.

Given a proton (mass M) of energy T and momentum P , at an angle of θ with the photon direction (all in the laboratory system) the photon energy W is given by

$$W = 2T/[1 - T/M + P \cos\theta/M] \quad (16)$$

(here we are neglecting the binding energy of the deuteron).

For the transformation from the CM system to the laboratory system we shall also need the angle θ_c in the CM system in terms of the laboratory angle θ ; and we shall need the ratio $\gamma = v'/v'' =$ ratio of velocity of the CM system relative to the laboratory to proton velocity in the CM system. We can derive the relations

$$\sin\theta_c = (1 - T/M + P \cos\theta/M)^{1/2} \sin\theta, \quad (17)$$

$$\gamma = v'/v'' = [(W/4Mc^2)(1 + 3W/4Mc^2)]^{1/2}. \quad (18)$$

The differential cross section for proton production in the CM system is given by SMG as

$$d\sigma/d\Omega = (3/8\pi)\sigma_1(W) \sin^2\theta_c [1 + (20\sigma_2/\sigma_1)^{1/2} \cos\theta_c + 5(\sigma_2/\sigma_1) \cos^2\theta_c]. \quad (19)$$

For neutron production the interference term changes sign.

$$d\sigma'/d\Omega = (3/8\pi)\sigma_1(W) \sin^2\theta_c [1 - (20\sigma_2/\sigma_1)^{1/2} \cos\theta_c + 5(\sigma_2/\sigma_1) \cos^2\theta_c]. \quad (20)$$

In Eqs. (19) and (20), σ_1 is the total cross section for the electric dipole term [see Eq. (12)] and σ_2 for the electric quadrupole term. SMG's results can be represented within 10 percent accuracy, by the convenient relation

$$\sigma_2/\sigma_1 = 1.16\gamma^2. \quad (21)$$

The transformation from CM system (θ_c) to laboratory system (θ) is made using Eq. (17) to rewrite all functions of θ_c in terms of θ . We also use the factor for transformation of the solid angle²⁵

$$(d\sigma/d\Omega)_{\text{Lab}} = (d\sigma/d\Omega)_{\text{CM}} (1 + 2\gamma \cos\theta_c + \gamma^2)^{3/2} / (1 + \gamma \cos\theta_c). \quad (22)$$

Since measurements are made for constant proton energy T we have the third factor discussed above giving a forward angular distribution. This factor is the product of the photon absorption cross section, $\sigma_1(W)$, and the photon distribution in the incident beam. We take dW/W (an approximation to the bremsstrahlung spectrum) as the photon distribution, which corresponds

²⁵ See, for example, L. I. Schiff, *Quantum Mechanics* (McGraw-Hill Book Company, Inc., New York, 1949), Sec. 18.

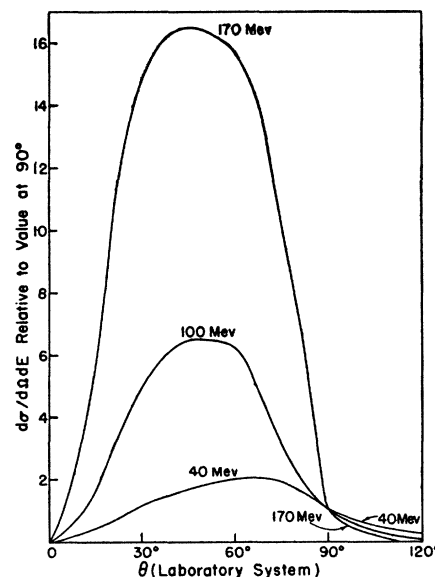


Fig. 1. Angular distribution of protons from deuteron photodisintegration.

to a beam intensity of one "Q." (The beam intensity in units of "Q" is defined as the ratio of the total energy in the beam to the energy of the most energetic photon.) Using Eq. (12) for σ_1 , the third factor can be written

$$\sigma_1 dW/W = 18.3 [1 - y^2(44 + y)^{-2}]^2 (y - 1)^{1/2} y^{-3} dW/W \quad (23)$$

where $y = W/\epsilon$.

This gives us the cross section per differential photon energy dW . To convert to the cross section per differential proton energy dT , we use

$$d\sigma/d\Omega dT = (d\sigma/d\Omega dW)(dW/dT). \quad (24)$$

The results for the deuteron photodisintegration, using Eqs. (16) through (24), are shown in Figs. 1, 2, and 3. Figure 1 shows the angular distributions in the laboratory system for protons of 40 MeV, 100 MeV, and 170 MeV, expressed as ratios of the differential cross section to that at 90°. The angular distribution is markedly forward, even for proton energies as low as 40 MeV; and is very strongly peaked forward for higher proton energies. Since we are including only photoelectric transitions, the cross section falls to zero for 0°, and also for 180°.

The differential energy spectrum for emitted protons is drawn with a log-log scale in Fig. 2 for laboratory angles of 30°, 90°, and 120°. The calculated results can be represented by a power law in the relevant energy range: $d\sigma$ is proportional to T^{-n} . For $\theta = 30^\circ$, $n = 2.5$; for $\theta = 90^\circ$, $n = 4.4$; for $\theta = 120^\circ$, $n = 6.5$. The energy spectrum becomes very steep for larger angles, since at

²⁶ Note that a differential cross section for 100-Mev protons at 30° of 0.015 microbarn/steradian Mev per Q corresponds to a much larger cross section per photon. A Q value of unity means that there are only 2/200 = 1/100 photon in the range 200 to 202 Mev, which corresponds to protons in the range 100 to 101 Mev.

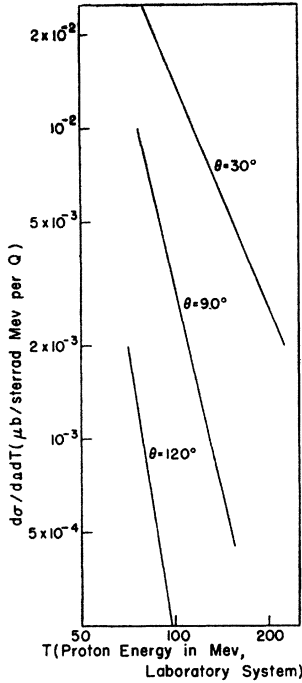


FIG. 2. Differential energy spectrum of protons from deuteron photodisintegration.

higher energies the angular distribution becomes extremely strongly forward.

Both Fig. 1 and Fig. 2 are drawn for a photon spectrum dW/W with no upper limit on the photon energy. Calculations in this paper apply to upper limits of 200 Mev, and 300 Mev, respectively. For the upper limit of 200 Mev, and for $T = 100$ Mev the angular distribu-

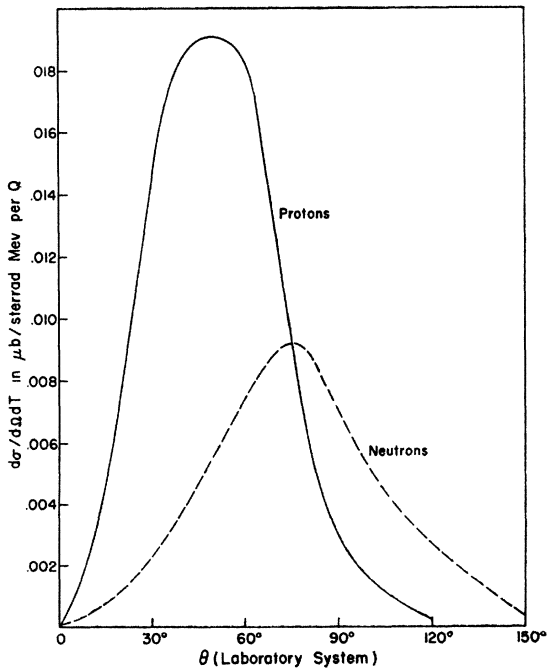


FIG. 3. Angular distribution for protons and neutrons from deuteron photodisintegration.

tion of Fig. 1 should go to zero for a laboratory angle of 80° , and there will be no protons at all of energy 170 Mev. The cutoffs for the angular and energy distributions are shown in Table I, which is based on Eq. (16).

Figure 3 compares the differential cross sections for proton production and for neutron production, at energies of 100 Mev. (The cutoff shown in the second line of Table I applies to the angular distribution.) The neutron distribution is only moderately forward since the dipole-quadrupole interference term provide a backward asymmetry canceling much of the forward asymmetry due to motion of the CM system. The angular distributions of protons and neutrons are more alike for lower energies, and differ more widely than those of Fig. 3 for higher energies.

V. THE NUCLEAR PHOTOEFFECT

The general features of the angular distributions and energy spectrum of the deuteron photoeffect persist in the calculation of the nuclear photoeffect; but they are shifted in energy, and somewhat smeared out, due to the influence of the remainder of the nucleus.

First, the quasi-deuterons in the nucleus have a

TABLE I. Cutoff due to upper limit on photon spectrum.

Proton energy:	for $W_{\max} = 200$ Mev	for $W_{\max} = 300$ Mev
$T = 40$ Mev	all angles possible	all angles possible
$T = 100$ Mev	$\theta_{\max} = 80^\circ$	$\theta_{\max} = 120^\circ$
$T = 170$ Mev	no angles possible	$\theta_{\max} = 60^\circ$
Angle of observation:		
$\theta = 30^\circ$	$T_{\max} = 135$ Mev	$T_{\max} = 210$ Mev
$\theta = 90^\circ$	$T_{\max} = 90$ Mev	$T_{\max} = 130$ Mev
$\theta = 120^\circ$	$T_{\max} = 72$ Mev	$T_{\max} = 98$ Mev

positive energy, corresponding to the wave number k , of Eq. (3). While there is a spread from 0 to 40 Mev in the positive energy, the effects of this spread are much smaller than the smearing effects of motion of the quasi-deuteron discussed below, and shall be neglected. We take the average positive energy as 12 Mev.

Correcting for this effect gives us the differential cross section for proton production, against proton angle and proton energy, for protons still in the nucleus. The proton energy in the laboratory is less than that inside the nucleus by the depth of the nuclear potential well, which is about 30 Mev for a typical nucleus.²⁷ The positive energy of the quasi-deuteron, and the nuclear potential shift the energy scale used in Fig. 2 for the deuteron photoeffect by 18 Mev.

²⁷ The nuclear potential well is a somewhat uncertain concept at high nuclear energies, as is indicated by recent work on scattering of high energy neutrons. [Fox, Leith, Wonters, and MacKenzie, Phys. Rev. **80**, 23 (1950); and J. DeJuren, Phys. Rev. **80**, 27 (1950)]. For example, it is not clear whether the potential well for a tightly bound nucleus, such as C^{12} , is deeper than that for a more typical nucleus. We shall use the value of 30 Mev. Our results are rather sensitive to the assumed depth of the potential well, since the proton energy spectrum is so steep. Thus a 10-Mev change in the assumed well depth, for proton energies of 100 Mev, causes about a 30 percent change in calculated differential cross section for 100-Mev protons.

The effects of the motion of the quasi-deuteron in the nucleus can be considered in terms of the components of its velocity: v_x along the direction of observation, and v_y perpendicular to the direction of observation, but in the plane formed by the photon direction and the direction of observation. $v_x = \frac{1}{2}(v_{1x} + v_{2x})$ where v_{1x} and v_{2x} are velocity components for the two nucleons when far apart from each other. (The third component v_z is not important for our present work.) The component v_x changes the observed energy, while v_y changes the observed angle. We shall make the approximation of considering that v_x and v_y have uncorrelated probability distributions. We shall make the further approximation that both v_x and v_y have the "triangular" probability distribution given in Eq. (25) and shown as the solid line in Fig. 4. (It would be more accurate to use the probability distribution for v_x given by the Fermi distribution for a nuclear temperature of about 8 Mev. This is sketched as the dotted curve in Fig. 4.) We use

$$P(v_x) = \begin{cases} (1 - |v_x/v_m|)/v_m, & |v_x| \leq v_m \\ 0 & |v_x| \geq v_m. \end{cases} \quad (25)$$

Here v_m is the maximum velocity for a nucleon in a nucleus, which corresponds to a maximum kinetic energy of 20 Mev.

Consider a proton which outside the nucleus has energy T , and velocity v_1 . It could have been produced with velocity $v'' = v_1 - v_x$, (and energy T'') from a quasi-deuteron which had velocity component v_x towards the observer. The differential cross section for production of a proton of energy T , is the differential cross section for production of protons of energy T'' , convoluted with the probability distribution for v_x .

$$d\sigma(T) = \int d\sigma(T'')(dT''/dT)P(v_x)dv_x. \quad (26)$$

The component of motion v_y affects the direction in which the proton is observed. A proton produced at angle $\theta' = \theta - \varphi$ is observed at angle θ , where

$$\varphi = \tan^{-1}(v_y/v_1) = v_y/v_1. \quad (27)$$

The differential cross section, as a function of θ , is multiplied by the probability distribution for v_y , and integrated over all angles.

$$d\sigma(\theta) = \int d\sigma(\theta')(\sin\theta'/\sin\theta)P(v_y)dv_y. \quad (28)$$

The correction factors for the cutoff of the photon spectrum, at energy W_{\max} , combined with the integrals of Eq. (26) and Eq. (28) for the motion of the quasi-deuteron, are expressed as a correction factor M , multiplying the differential cross section for a deuteron at rest, with no cutoff on the photon spectrum. The motion of the quasi-deuteron tends to smooth out the angular distribution shown in Fig. 1 for a deuteron at rest since factor M is small for the peak of the angular dis-

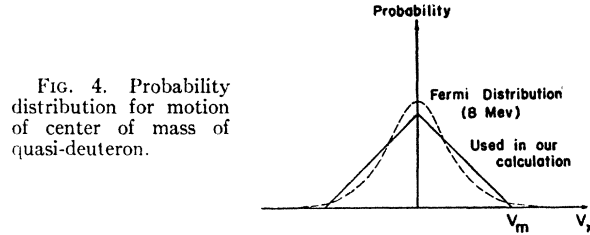


FIG. 4. Probability distribution for motion of center of mass of quasi-deuteron.

tribution and becomes larger for both large and small angles. The principal effect on the energy spectrum is that appreciable numbers of protons are observed at energies above the sharp cutoff which would be observed for a quasi-deuteron at rest. However, the energy spectrum decreases much more rapidly for energies above the cutoff than for energies below the cutoff.

Using the factor $6.4 NZ/A$ of Eq. (10) for the carbon nucleus, together with the correction factor M discussed above, and the differential energy spectrum for protons produced by deuteron photodisintegration (Fig. 2), we find the differential energy spectrum shown in Fig. 5 for laboratory angles of 30° and 90° . The solid curves are for a photon cutoff at 200 Mev photon energy; the dotted curves for 300 Mev maximum photon energy. While Fig. 2 shows a power law energy spectrum, Fig. 5 shows a spectrum similar to a power law for energies below the cutoff, but decreasing much more rapidly at higher photon energies. The arrows indicate the proton cutoff energies that would be observed if there were no motion of the quasi-deuteron. Expressed as cross sections per Q , the cross sections for 200 and 300 Mev maximum photon energy are nearly the same for proton energies below the lower proton cutoff.

VI. COMPARISON WITH EXPERIMENT

Levinthal and Silverman¹ measured protons produced by photons from the 300-Mev Berkeley synchrotron.

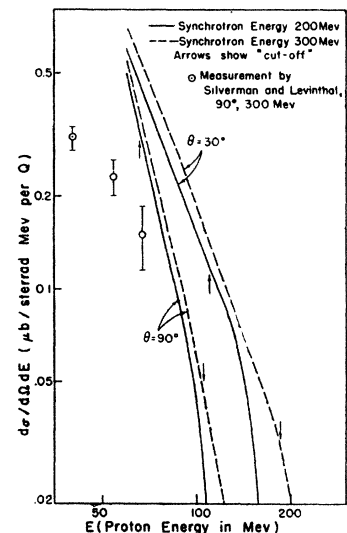


FIG. 5. Differential energy spectrum protons from carbon.

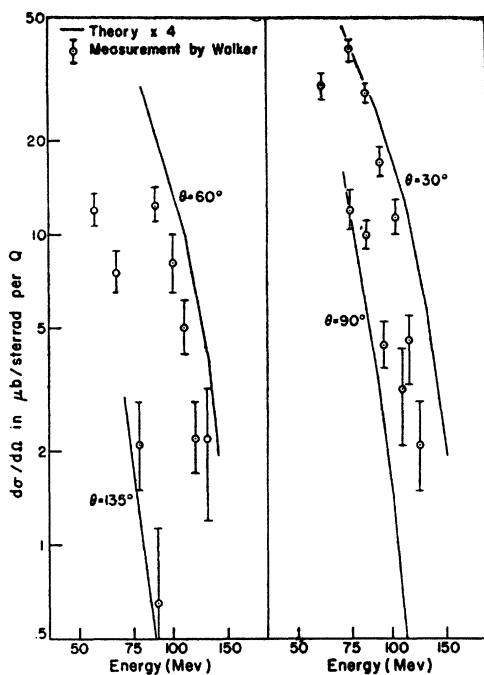


FIG. 6. Integral energy spectrum protons from carbon.

They used proportional counters to measure protons at the end of their range, thus obtaining a differential energy spectrum. Their experimental results for protons from carbon at 90° , in the laboratory system, are compared with our calculations in Fig. 5. The experimental points should be compared with the lower dotted curve.

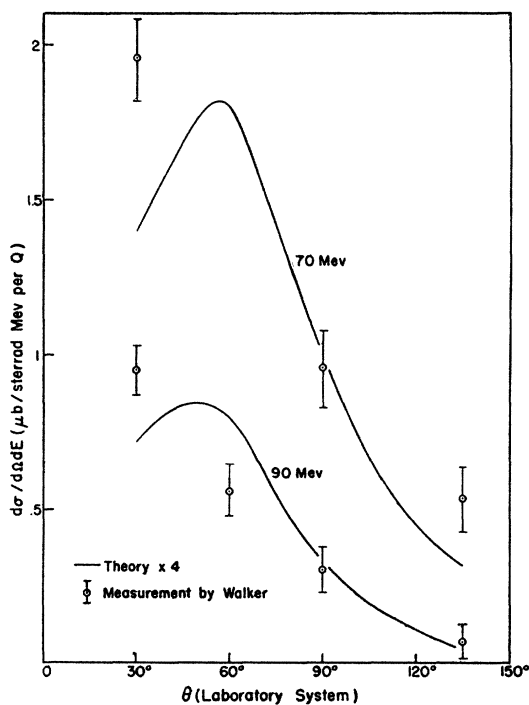


FIG. 7. Angular distribution protons from carbon.

We observe that the absolute cross section calculated at 67 Mev is about twice that measured by Levinthal and Silverman. The calculated energy spectrum is a much more rapidly varying function of proton energy than is the experimental energy spectrum. These discrepancies are not unexpected, since our method of calculation (setting the overlap integral for $\phi(3 \cdot \cdot \cdot A) = 1$ will overestimate the cross section and the error would be worse at low photon energies, where the quasi-deuteron model becomes poor.

Levinthal and Silverman¹ also measured the angular distribution for 40-Mev protons. They found that the differential cross sections at laboratory angles of 45° , 90° , and 135° had the ratios 1.6, 1, and 0.6. Our calculations do not extend to this low a proton energy. However their result is in qualitative agreement with the angular distribution of Fig. 2.

They also measured proton production from elements from beryllium to lead, and found that the cross section was proportional to Z .

Walker³ has measured high energy protons from carbon by the Cornell synchrotron operating at 200 Mev. He used a photographic emulsion technique, which gives him an integral energy spectrum. That is, he measured $d\sigma/d\Omega$ for protons of energy greater than E_0 . To compare with his results, we have integrated the differential energy spectrum shown in Fig. 5, and other similar curves at other angles. Figure 6 compares Walker's integral energy spectrum²⁸ with our calculated result for laboratory angles of 135° , 90° , 60° , and 30° . To facilitate the comparison we have multiplied our theoretical cross sections by a factor of four. We find fair agreement in the shapes of the curves between theory and experiment over a wide range of energies and angles. The probable errors are only those for relative measurements.

In Fig. 7 we compare the angular distribution for the differential energy spectrum, at proton energies of 70 Mev and 90 Mev, with values found by Walker. Again we have multiplied the calculated cross sections by the factor of four to facilitate comparison. We find fair agreement between theory and experiment in the shape of the angular distribution. Apparently the cross section measured experimentally rises from 60° to 30° , while the calculated cross section falls slightly. Also the measured cross section does not fall quite so low as the calculated cross section at 135° . The probable errors of the measurements are not small enough to establish these discrepancies. We shall suggest below possible causes for these discrepancies.

Keck² measured protons produced by the Cornell synchrotron operating at 300 Mev. He measured protons at the end of their range using scintillation counters. As his results are still preliminary, we shall

²⁸ Note that, because of the recalibration of the photon intensity at the Cornell synchrotron, by J. DeWire and J. Keck, Walker's published results [Phys. Rev. **81**, 634 (1951)] have been divided by the factor 1.44.

quote only their general features, to compare with the calculations of this paper. Keck measured the differential energy spectrum of protons from carbon, at $67\frac{1}{2}^\circ$ in the laboratory system, for proton energies from 70 Mev to 240 Mev. The absolute cross section was about twice that calculated in this paper. Keck measured the angular distribution for angles from 15° to 120° , at proton energies of 95, 125, and 175 Mev. His measurements show the same discrepancies between calculations and experiment indicated by Walker's angular distribution, i.e., the calculations give too low a cross section both at very small angles, and at very large angles.

Like Levinthal and Silverman, Keck found that the photoproton yield was proportional to Z . Our calculations give a photoproton yield proportional to NZ/A , which is very close to proportional to A , and therefore increases somewhat more rapidly than Z . This more rapid increase with Z is counteracted by the probability of escape of the photoproton from the nucleus, which is a decreasing function of Z .

The measurements on photoprotons from carbon by Levinthal and Silverman, Walker, and Keck overlap at a proton energy of 70 Mev and angle of 90° . Their absolute values for this differential cross section are compared with each other, and with our calculation, in Table II. (Keck's measurement at $67\frac{1}{2}^\circ$ are divided by a factor 1.5, based on Walker's angular distribution, to convert to a cross section at 90° .) The agreement among the experimental measurements of the absolute cross section is fair: i.e., not very far outside the maximum likely errors of measurement. The agreement between our calculations and the experiments is within the estimated errors.

Keck also used an organic scintillation counter to measure high energy photoneutrons from carbon. He found that their number agreed in order of magnitude with the number of high energy photoprotons.

Keck has measured some coincidences between high energy neutrons and protons, and finds some correlation between their directions of emission. The coincidence rate was much smaller than the single counting rate for high energy nucleons. Presumably this is the result of "smearing effects" such as motion of the quasi-deuteron, and scattering of the emitted neutron and proton. A detailed comparison between experiment and calculations from the deuteron model has not yet been made. Keck's observation of neutron-proton coincidences appears to be the crucial experiment in establishing the deuteron model for nuclear processes at very high excitation energy.

TABLE II. Comparison of absolute cross sections.

Worker	Method	Synchrotron energy	$d\sigma/d\Omega dE$ in $\mu\text{b/sterad Mev per } Q$	Maximum likely error
Levinthal and Silverman	Proportional counter	300 Mev	0.15	factor of 2
D. Walker	Photographic emulsion	200 Mev	0.95	55%
J. Keck	Scintillation	300 Mev	0.74	30%
J. Levinger	Calculation	200 Mev	0.25	factor of 3
J. Levinger	Calculation	300 Mev	0.29	factor of 3

There is also some evidence for neutron proton coincidences from the cloud chamber pictures by Gaerttner and Yeater.²⁹ They believe that the (γ, pn) process is the predominant mode of disintegration for nitrogen by the photon beam from the 100-Mev G.E. betatron.

The calculations of this paper have omitted various effects that might advantageously be considered in a more detailed treatment. We have taken no account of scattering of the high energy photoproton by other nucleons in the nucleus. This will tend to change the directions of some high energy protons, making for a more isotropic distribution in the laboratory system, and, particularly for large nuclei, will prevent the emission of some high energy protons. In correcting for the motion of the quasi-deuterons, one might use the Fermi distribution for 8 Mev sketched in Fig. 4, instead of the probability distribution used in this paper.

The process of meson emission and reabsorption to produce high energy protons is negligible for measurements with 200-Mev maximum photon energy since the cross section for meson production is so small at these energies, but it might be appreciable for higher photon energies. This is another process tending to give an angular distribution more isotropic in the laboratory system.

Finally, we have used an incomplete calculation of the deuteron photoeffect. If there are appreciable photomagnetic cross sections, this would give a significant increase in the cross section for small angles, in the laboratory system.

The author is grateful to H. A. Bethe, E. Salpeter, and J. Heidmann for discussions of theoretical aspects of this problem; and to A. Silverman, S. Kikuchi, J. Keck, and D. Walker for communication and discussion of their experimental results. Part of this work was done while the author was employed under an ONR contract.

²⁹ Gaerttner and Yeater, Phys. Rev. **77**, 714 (1950).